NANOSYSTEMS: PHYSICS, CHEMISTRY, MATHEMATICS, 2017, 8 (6), P. 816–822

Stable Ti_9O_{10} nanophase grown from nonstoichiometric titanium monoxide TiO_y nanopowder

A. A. Valeeva[1,2], M. G. Kostenko[1]

[1]Institute of Solid State Chemistry, Ural Branch of the Russian Academy of Sciences,
620990 Pervomayskaya 91, Ekaterinburg, Russia
[2]Ural Federal University named after the first President of Russia B. N. Yeltsin,
620002 Mira 19, Ekaterinburg, Russia
anibla_v@mail.ru, makskostenko@yandex.ru

PACS 61.72.Dd, 61.72.Bb, 64.70.Nd, 71.20.Ps **DOI 10.17586/2220-8054-2017-8-6-816-822**

A new stable Ti_9O_{10} nanophase (sp. gr. *Immm*) has been detected by X-ray diffraction (XRD) after high energy ball milling and long-term vacuum annealing of nanocrystalline powder of nonstoichiometric disordered and ordered titanium monoxide TiO_y with $B1$ structure (sp. gr. $Fm\bar{3}m$). With the help of XRD data, the unit cell of the Ti_9O_{10} nanophase as well as the distribution of atoms and structural vacancies in the titanium and oxygen sublattices of this phase have been established. The crystal structure of Ti_9O_{10} is derived from that of TiO_y by (a) a migration of the vacancies to the specific crystallographic planes of $B1$ structure and (b) by orthorhombic distortions. The DFT calculations of the full energy of the coarse-crystalline phases TiO_y and Ti_9O_{10} revealed that the bulk ordered phase Ti_9O_{10} is not preferable in comparison with the bulk disordered cubic phase TiO_y with the same content of vacancies in the sublattices, so, it is the nanostate that causes the formation of Ti_9O_{10}.

Keywords: Titanium monoxide, ball milling, nanophase Ti_9O_{10}, phase transition, electronic structure.

Received: 22 October 2017

Revised: 27 October 2017

1. Introduction

In the titanium–oxygen system there are many nonstoichiometric phases [1], which are interesting from both fundamental and practical standpoints. For the examination and application of nonstoichiometry, special attention is given to nonstoichiometric titanium monoxide TiO_y having a wide homogeneity range from $TiO_{0.70}$ to $TiO_{1.25}$ and a high content of structural vacancies in the titanium and oxygen sublattices of the basic $B1$ structure [2–4]. Structural vacancies are an inherent part of the structure of titanium monoxide. They determine the concentration and temperature order-disorder phase transitions [5]. There is substantial documentation in the literature regarding the formation of different ordered phases with cubic, tetragonal, orthorhombic, hexagonal and monoclinic lattices [4–10]. The literature data are only available for coarse-crystalline state and often contradict each other. It is known that in titanium monoxide of stoichiometric composition $TiO_{1.0}$, at temperatures below 1263 K, a monoclinic superstructure is formed [4, 6], while at temperatures from 1253 to 1523 K, a cubic ordered phase exists [6]. In work [7], a model of cubic Ti_5O_5 superstructure is proposed. The unit cell has a triple spacing as compared with the unit cell of the basic $B1$ structure. Recently [8] a new polymorph of titanium monoxide, ε-TiO, was synthesized. The single crystals of ε-TiO [8] have a hexagonal structure (sp. gr. $P\bar{6}2m$), which is not $B1$ derived but, according to the calculations, is more stable than the ordered monoclinic phase [4,6]. For compositions ranging from $TiO_{0.7}$–$TiO_{0.9}$ at the temperatures higher than 873 K, an orthorhombic superstructure ($I222$) was reported [2]. However, according to [9], titanium monoxide of substoichiometric composition contains only one ordered phase with monoclinic structure (sp. gr. $C2/m$ or ($A2/m$)). In the range $TiO_{1.00}$–$TiO_{1.50}$, the following ordered phases were found: the orthorhombic phase $TiO_{1.20}$ (sp. gr. *Immm*, *Imm*2 or $I222$) stable below (or at) 1093 K and the tetragonal phase $TiO_{1.25}$ (sp. gr. $I4$/m, $I4$ or $I\bar{4}$) stable below 993 K [6].

The powder standard database (card ICSD #77698) contains a calculated powder XRD pattern for Ti_9O_{10} phase (sp. gr. *Immm*) with crystal structure parameters from work [6]. However, in [6], the Ti_9O_{10} is not mentioned. On the latest Ti–O phase diagram, the Ti_9O_{10} phase (sp. gr. *Immm*) is also lacking [1]. Thus, at present, we have only to deal with the calculated Ti_9O_{10} structure and there is no information about the experimentally grown Ti_9O_{10} phase.

Recently, increasing attention is being given to study the effect of small particle size on the stability, properties, nonstoichiometry and structural characteristics of the compounds during the transition from a microcrystalline state to a nanocrystalline one (see [11–13] for example). The nanocrystalline state is far from equilibrium because

of the particles' large specific surface area and excessive free energy, which is a prerequisite for varying the thermodynamic characteristics of the system and its properties as a whole. The nanostate offers vast opportunities for creating a large variety of properties of materials without changing their chemical composition but changing the size of particles and the manner of atomic ordering [12].

In this regard, the aim of this work was the determination of the changes in titanium monoxide's crystal structure during its transition from a coarse crystalline state to a nanocrystalline one.

2. Material and methods

The coarse crystalline samples of titanium monoxide $TiO_y \equiv Ti_xO_z$, where $y = z/x$, with an average size of about 25 μm were synthesized by solid-phase sintering from a mixture of titanium Ti and titanium dioxide TiO_2 powders in vacuum of 10^{-3} Pa at 1773 K. The synthesized samples of titanium monoxide contained two phases – disordered cubic phase (sp. gr. $Fm\bar{3}m$) and ordered monoclinic phase (sp. gr. $C2/m$). In order to attain the disordered state, the samples were annealed in vacuum for 3 h at 1373 K, which exceeds the temperature of the equilibrium order-disorder transition. Whereupon the ampoules with the samples were dropped into water, the quenching rate was about 200 K/s. Analysis of the XRD pattern showed that complete disordering in the samples was not reached, partial ordering retained, and the long-range order degree η of the quenched samples was 0.21 [14]. To achieve the ordered state, low-temperature annealing was carried out at 673 K for 4 h in evacuated (10^{-3} Pa) quartz ampoules. After such annealing, the ampoules were slowly cooled to ambient temperature. Analysis of the XRD patterns revealed that annealing at 673 K allowed production of samples with the long-range order degree of $\eta = 0.62$. Multiparameter characterization of the samples was performed by chemical, spectral, picnometer, X-ray phase and X-ray structural analyses [10, 15].

Nanocrystalline titanium oxide powders were produced by high-energy ball milling of coarse crystalline titanium monoxide powders in a Retsch PM 200 planetary-type ball mill. The material of the mill balls and cups was zirconium dioxide ZrO_2 stabilized by yttrium oxide Y_2O_3. The mass ratio between the mill balls and the powder was 10:1. Isopropyl alcohol was used as a milling liquid, the rotation velocity of the backing plate of the mill cups was 500 rpm, the duration of milling was 480 min. Along with particle size reduction owing to grinding crystal lattice, microstrains appeared in the nanoparticles. The small size and microstrain contributions to the reflection broadening in XRD patterns were determined by the Williamson–Hall method [16, 17]. Owing to the fragmentation of ordered titanium monoxides with near stoichiometric composition, nanoparticles of 20 ± 10 nm in size with the least microstrains of about 0.3 % were prepared. During the fragmentation of the disordered titanium monoxides both with sub- and superstoichiometric compositions, the particle sizes were approximately the same, but the microstrains increased by 3 fold. The method for the preparation of nanoparticles by high-energy milling, analysis of XRD patterns and determination of the coherent scattering regions were reported in detail in [18].

XRD studies of the powders were performed in Cu$K\alpha_1$-radiation on a STADI-P automatic diffractometer (STOE, Germany) in the Bragg–Brentano geometry by stepwise scanning with $(2\theta) = 0.02$ in the 2 angle interval from 10 to 120 with a high degree of statistics. Polycrystalline silicon ($a = 543.07$ pm) was used as external standard. Phase analysis of the XRD pattern was performed using Powder Cell 2.4 program. For phase identification the powder standards database ICDD PDF2 (ICDD, USA, Release 2009) was used.

The long-range order parameters of the ordered monoclinic phase were calculated on the basis of the full-profile analysis results by analyzing of the variation in the intensity of structural and superstructural reflections before and after heat treatment.

Experiments on annealing of the titanium monoxide nanopowders were performed from 300 to 1200 K in vacuum of about 10^{-3} Pa with long-term exposure for complete termination of the processes in the system and for structure stabilization. The heating and cooling rate was about 1 K/min. After each exposure, we carried out the X-ray phase analysis to estimate the structural changes occurring after the annealing.

The electronic structure and stability of the bulk Ti_9O_{10} phase were studied using first-principles calculations. The results were compared with the disordered phase of the same composition $TiO_{10/9}$. The calculations were carried out in the framework of the density functional theory [19, 20] with allowance for the exchange-correlation potential in the generalized gradient approximation (GGA) of the PBE version [21]. The PWSCF code of the Quantum ESPRESSO software suite [22] based on the plane wave and pseudopotential method was used. The energy of the plane waves did not exceed 45 Ry. Besides the valence $3d4s$ states, the semi-core $3s3p$ states were included into the titanium pseudopotential.

3. Results

3.1. The results of the experiment and discussion

Analysis of the XRD pattern of the initially quenched coarse crystalline titanium monoxide sample of stoichiometric composition ($TiO_{1.00}$) revealed that the sample contains two phases with $B1$ derived structures: cubic TiO_y (sp. gr. $Fm\bar{3}m$) with disordered distribution of the structural vacancies and the ordered monoclinic Ti_5O_5 (sp. gr. $C2/m$), the long-range order parameter η being equal to 0.21 [14]. After long-term heating from ambient temperature to 1200 K, the reflection intensity of the ordered phase Ti_5O_5 on the XRD pattern has increased. Analysis of the variation in intensity of the structural and superstructural reflection showed that the long-range order parameter reached a value of $\eta = 0.54$. Thus, slow heating to high temperatures and slow cooling to ambient temperature made it possible to increase the long-range order degree in the sample with initial strong vacancy disordering.

According to analysis of the experimental XRD patterns, the annealed crystalline titanium monoxide in the initial state also contained two phases: cubic TiO_y (sp. gr. $Fm\bar{3}m$) and monoclinic Ti_5O_5 (sp. gr. $C2/m$) (Fig. 1*a*). After the series of long-term heating the structure of the sample remained monoclinic. Slow annealing to high temperatures and slow cooling to ambient temperature allowed an increase in the long-range order degree in titanium monoxide from 0.62 to 1.00, which corresponds to the maximal long-range order degree.

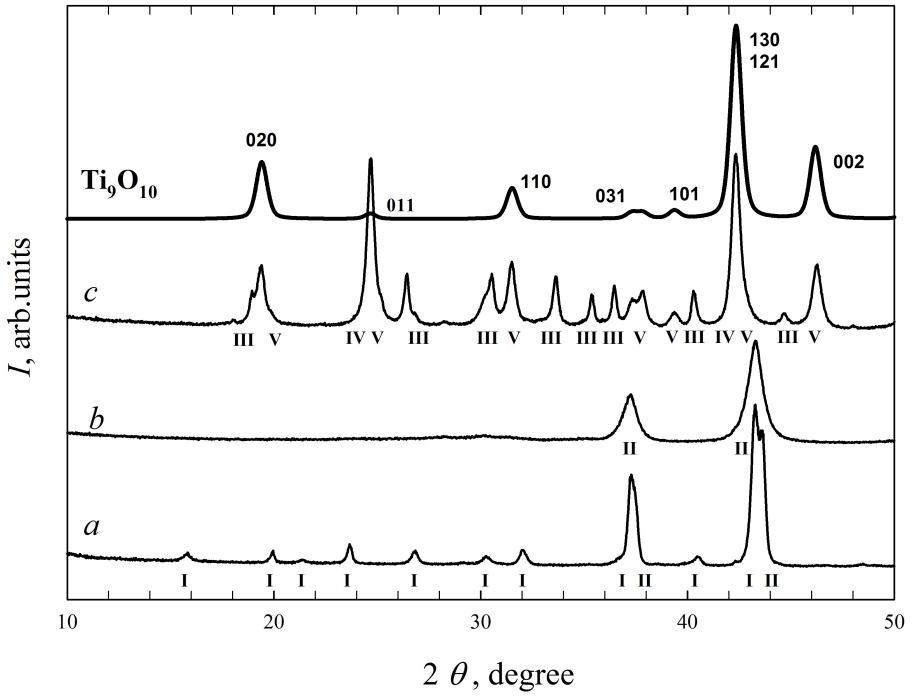

FIG. 1. The XRD patterns of the titanium oxide powders at ambient temperature: a) initial microcrystalline annealed powder (phases: I – Ti_5O_5, II – TiO_y); b) milled nanocrystalline annealed powder (II – TiO_y phase); c) powder annealed at 1200 K and quenched from 1200 K to ambient temperature (phases: III – Ti_3O_5, IV – Ti_9O_{10}, V – TiO_2). Calculated XRD pattern of Ti_9O_{10} (upper pattern). Additionally the reflection Miller indices for the Ti_9O_{10} phase are shown

For annealed and quenched nanocrystalline titanium monoxide TiO_y, we have observed different effects. The initial annealed nanocrystalline sample prepared by high-energy milling contained exclusively the cubic phase TiO_y (Fig. 1*b*). Analysis of the XRD pattern showed that milling leads to disordering and to the lowering of the long-range order degree. Long term vacuum annealing of nanopowder of the ordered titanium monoxide to 1200 K (Fig. 1*c*) gives rise to the following phases: Ti_9O_{10} (sp. gr. *Immm*) – 50 mass %, Ti_3O_5 (sp. gr. *I*2*c*) – 20 mass % and TiO_2 (anatase) – 30 mass %. Quenching of the samples from 1200 K to ambient temperature no longer transforms the sample into the initial cubic state.

Long term vacuum annealing of quenched titanium monoxide nanopowder leads, already at 673 K, to partial oxidation of titanium monoxide and, according to the X-ray structural analysis, 3 phases co-exist in the system

TABLE 1. Bond lengths (pm) and bond angles (deg.) in Ti_9O_{10} nanophase

Ti2*a*–O2*c*	196.3	O2*c*–Ti2*a* –O2*c*	180
		O2*c*–Ti2*a* –O4*h*	90
Ti2*a*–O4*h*	196.3	O4*h*–Ti2*a* –O2*c*	44.32
		O4*h*–Ti2*a* –O2*c*	45.68
Ti4*g*–O2*c*	213.7	O2*c*–Ti4*g* –O2*c*	44.32
		O4*h*–Ti4*g* –O2*c*	90
		O4*h*–Ti4*g* –O2*c*	180
Ti4*g*–O4*h*	196.3	O4*h*–Ti4*g* –O4*h*	90
		O4*h*–Ti4*g* –O4*h*	180
Ti4*g*–O4*h*	213.7	O4*h*–Ti4*g* –O4*h*	44.32

simultaneously: 60 mass % TiO_y (sp. gr. $Fm\bar{3}m$), 25 mass % Ti_9O_{10} (sp. gr. *Immm*) and 15 mass % TiO_2 (anatase). As the temperature is raised to 873 K, the amount of the Ti_9O_{10} phase increases to 60 mass %, while at 1200 K the cubic phase disappears completely and the following phases are formed: Ti_9O_{10} (sp. gr. *Immm*) – 70 mass %, Ti_2O_3 (sp. gr. $R\bar{3}2/c$) – 2 mass % and TiO_2 (anatase) – 28 mass %.

The crystal structure of the experimentally observed Ti_9O_{10} nanophase is shown in Fig. 2. The observed crystal structure can be built up from initial $B1$ structure of the disordered phase TiO_y by (a) an ordering of the structural vacancies by their diffusional shifts to the selected specific crystallographic planes and (b) by orthorhombic distortions. The last effect causes the additional reflections on the XRD pattern of milled and annealed powder (Fig. 1). As a result of the ordering, vacancy planes composed of titanium 2(*a*) and oxygen 2(*c*) positions alternate with two vacancy free planes composed of titanium 4(*g*) and oxygen 4(*h*) positions. In the initial disordered phase, TiO_y vacancy planes cannot be defined as the probability of finding a vacancy for all the sites are similar. In contrast to monoclinic and cubic Ti_5O_5 structures [4, 5, 7], the vacancy sites in Ti_9O_{10} are not 100 % completed with vacancies. The titanium 2(a) and oxygen 2(*c*) positions are filled with vacancies by 75 % and 50 %, respectively. The titanium 4(*g*) and oxygen 4(*h*) positions are completed with atoms.

There are six titanium and six oxygen sites in a unit cell. The lattice parameters are $a = 298.60$ pm, $b = 915.42$ pm, $c = 392.60$ pm, $\alpha = \beta = \gamma = 90$ °. The bond lengths and bond angles are presented in Table 1. The bond angles between nearest atoms of different types are equal to 44.32 °, 45.68 ° and 90 °. If the distortion of the basic $B1$ structure is not taken into account, the form of the Ti_9O_{10} unit cell and its position in the $B1$ matrix are similar to that of orthorhombic superstructures M_3X_2 and M_2X_3 (pr. gr. *Immm*) proposed in [23]. However, M_3X_2 and M_2X_3 contain vacancies in only one of the sublattices of the $B1$ structure (metal or nonmetal). In the structure of Ti_9O_{10}, the vacancies are available in both sublattices. Essentially, the structure of Ti_9O_{10} can be obtained with an overlapping of M_3X_2 and M_2X_3 superstuctures and a partial occupation of their vacancy sites with atoms.

3.2. The results of the first-principle calculations and discussion

The disorder in the arrangement of vacancies in the disordered phase $TiO_{10/9}$, as well as the disorder in vacancy planes of the Ti_9O_{10} structure (Ti 2(*a*) and O 2(*c*) positions) was simulated by a supercell method [24]. The supercells for both $TiO_{10/9}$ and Ti_9O_{10} were constructed by twofold translations of the orthorhombic unit cell of Ti_9O_{10} along the crystallographic directions *a*, *b* and *c* and contained 96 sites of $B1$ structure. The crystallographic positions *a* of the titanium sublattice in Ti_9O_{10} were randomly occupied by 12 vacancies, whereas positions *c* of the oxygen sublattice were randomly occupied by 8 vacancies. The number of vacancies in the titanium and oxygen sublattices in $TiO_{10/9}$ was the same as in Ti_9O_{10}. For each phase, 10 supercells with different random arrangements of vacancies were constructed. The results of calculation for 10 superstructures were averaged. Relaxation of the atomic positions was considered.

Figure 3 displays the partial densities of electronic states calculated for the disordered cubic phase of the composition $TiO_{10/9}$ (a) and for the Ti_9O_{10} phase (b). The changes in the electronic structure during the formation of Ti_9O_{10} manifest themselves mainly in the narrowing of the Ti 3*s*, Ti 3*p* and O 2*s* bands, as well as in the variation of the shape of the O 2*s* and O 2*p* bands. Additionally, the width of the *p*–*d* gap region between the O 2*p*

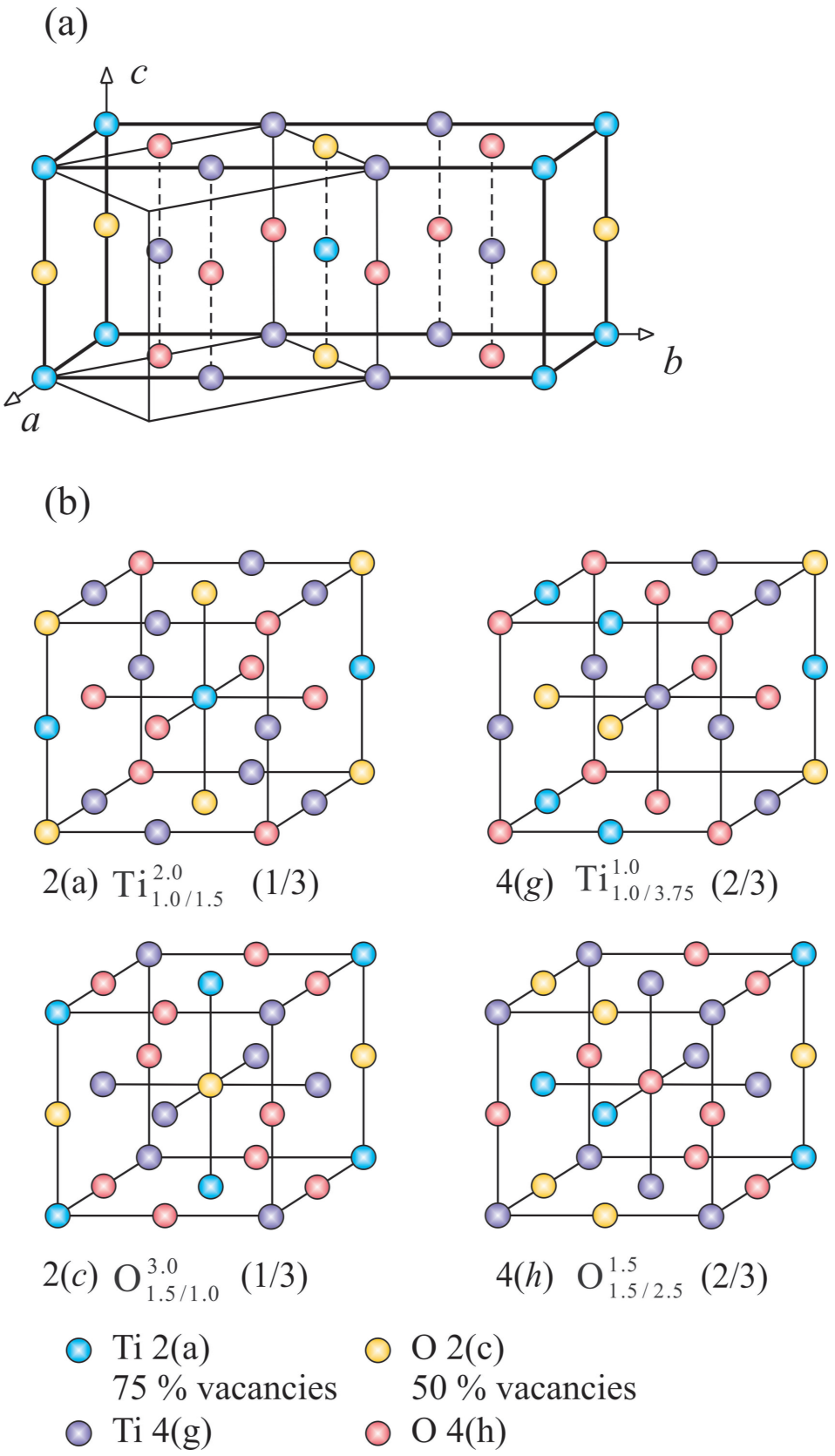

FIG. 2. The unit cell (bold line), the types of crystallographic positions and their multiplicity for the Ti_9O_{10} structure. The distorted unit cell of the B1 structure is indicated by tiny lines

and Ti 3*d* states in the Ti_9O_{10} structure is larger than that in the disordered cubic phase. Note that the dip in the density of Ti 3*d* states distribution for Ti_9O_{10} does not become more profound as compared with the disordered phase, which, according to [25–28], is typical of energetically favorable structures of titanium monoxide. On the other hand, complete disappearance of the dip occurring during the formation of energetically unfavorable local atomic vacancy correlations in the structure [29] is not observed either. The presence of the electronic states at the Fermi level is indicative of the metallic character of the considered phases.

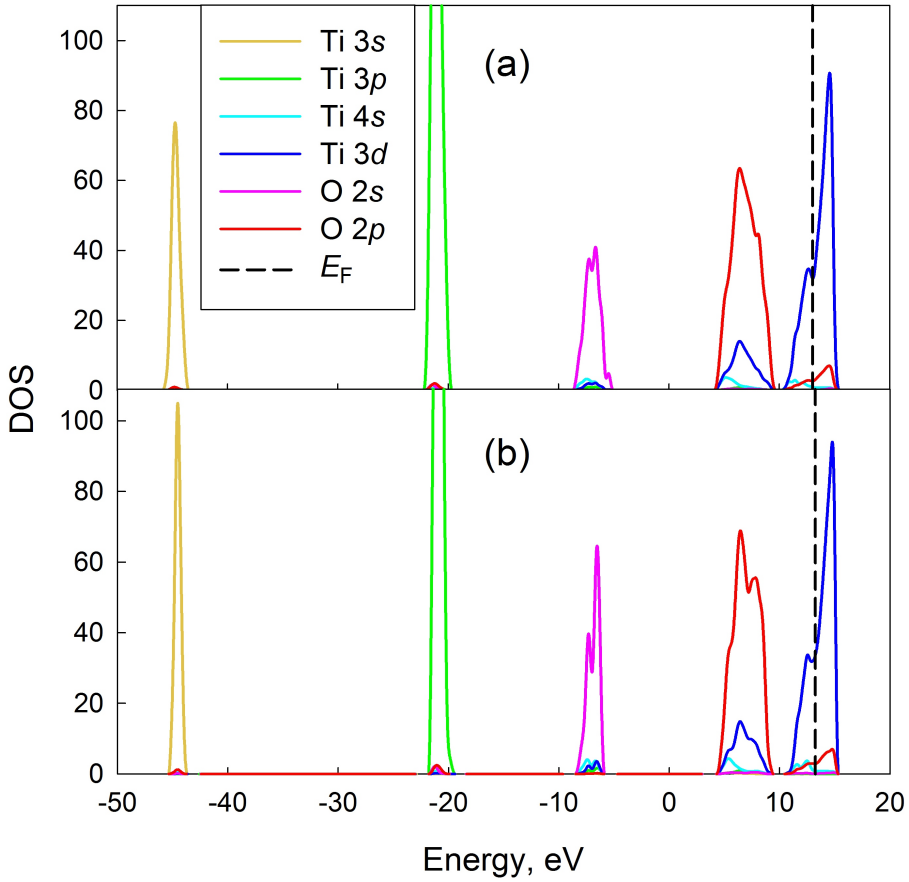

FIG. 3. The partial densities of electronic states calculated for the disordered cubic phase of the composition $TiO_{10/9}$ (a) and for the Ti_9O_{10} phase (b). The Fermi energy (EF) is indicated by a dotted line

As the energy characteristic of the phases the cohesive energy is calculated by the formula:

$$E_{coh} = \left(E - N_{\mathrm{Ti}} \cdot E_{\mathrm{Ti}} - N_{\mathrm{O}} \cdot E_{\mathrm{O}}\right) / N_{\mathrm{Ti_9O_{10}}}, \tag{1}$$

where E is the total energy of the phase examined per one supercell, N_{Ti}, N_{O} are the quantities of titanium and oxygen atoms in the supercell, respectively, E_{Ti}, E_{O} refers the total energy of a single Ti or O atom, and $N_{\mathrm{Ti_9O_{10}}} = 36$ is the number of $TiO_{10/9}$ structural units in the supercell. In the calculation of energies E_{Ti} and E_{O} the spin polarization effect was taken account. The cohesive energy of the disordered $TiO_{10/9}$ phase is equal to -14.35 ± 0.04, while the cohesive energy of Ti_9O_{10} phase turned out to be -14.34 ± 0.04 per formula unit. Thus, the formation of Ti_9O_{10} structure by distortion of the basic $B1$ structure and by variation of the concentration of disordered vacancies in certain crystallographic planes does not give any energy benefit in comparison to the disordered phase. As a matter of fact, the Ti_9O_{10} is the only experimentally confirmed ordered structure of titanium monoxide which ground state energy does not decrease in comparison with that of the disordered phase. We suppose it is the nanostate of the sample that causes the formation of the less energetically favorable ordered structure.

4. Conclusion

In this work, Ti_9O_{10} phase (sp. gr. *Immm*) has been synthesized by a long-term vacuum annealing of nanocrystalline titanium monoxide TiO_y at temperatures ranging from 300 to 1200 K. The unit cell for the Ti_9O_{10} phase has been found, established and constructed. The electronic structure and stability of the new Ti_9O_{10} phase have been studied using first-principle quantum-chemical calculations in comparison with the disordered phase of the same composition. The calculations showed that the Ti_9O_{10} phase is energetically unfavorable in a bulk state as compared with the cubic $B1$ structure. It is supposed that the Ti_9O_{10} phase is formed by transition from a crystalline state to a nanostate.

Acknowledgements

The work was carried out at the Institute of Solid State Chemistry UB RAS with financial support from the Russian Science Foundation (project 14-23-00025).

References

[1] Okamoto H. O–Ti (Oxygen-Titanium). *J. Phase Equil. Diffus.*, 2011, **32**, P. 473–474.
[2] Anderson S., Collen B., Kuylenstierna U., Magneli A. Phase Analysis Studies on the Titanium–Oxygen System. *Acta Chem. Scand.*, 1957, **11**, P. 641–1652.
[3] Banus M.D., Reed. T.B. Structural, electrical and magnetic properties of vacancy stabilized cubic TiO and VO. In: The Chemistry of Extended Defects in Non-Metallic Solids, Amsterdam-London: North-Holland Publ., 1970, P. 488–521.
[4] Watanabe D., Castles J.R., Jostson A., Malin A.S. Ordered Structure of Titanium Oxide. *Nature*, 1966, **210**, P. 934–936.
[5] Rempel A.A., Valeeva A.A. Thermodynamics of atomic ordering in nonstoichiometric transition metal monoxides. *Mend. Communication*, 2010, **20**, P. 101–103.
[6] Hilti E. Neue Phasen im System Titan–Sauerstoff. *Naturwissenschaften*, 1968, **55**, P. 130–131.
[7] Gusev A.I., Valeeva A.A. Diffraction of electrons in the Cubic Ti5O5 superstructure of titanium monoxide. *JETP Letters*, 2012, **96**, P. 364–369.
[8] Amano S., Bogdanovski D., et al. ε–TiO, a Novel Stable Polymorph of Titanium Monoxide. *Angew. Chem. Int. Ed.*, 2016, **55**, P. 1652–1657.
[9] Khaenko B.V., Kachkovskaya E.. Ordering and phase ratios in Ti–O system in the range of titanium monoxide existing. *Poroshkovaya metallurgiya (Powder metallurgy)*, 1986, **6**, P. 52–59.
[10] Valeeva A.A., Rempel A.A., Gusev A.I. Ordering of cubic titanium monoxide into monoclinic Ti_5O_5. *Inorganic materials*, 2001, **37**, P. 603–612.
[11] Valeeva A.A., Nazarova S.Z., Rempel A.A. Influence of Particle Size, Stoichiometry, and Degree of Long-Range Order on Magnetic Susceptibility of Titanium Monoxide. *Physics of the Solid State*, 2016, **58**, P. 771–778.
[12] Rempel A.A. Hybrid nanoparticles based on sulfides, oxides, and carbides. *Russ. Chem. Bull.*, 2013, **4**, P. 857–868.
[13] Schaefer H.-E. *Nanoscience*. Springer Verlag, Berlin, 2010, 772 p.
[14] Valeeva A.A., Nazarova S.Z., Rempel A.A. In situ study of atomic-vacancy ordering in stoichiometric titanium monoxide by the magnetic susceptibility. *JETP Letters*, 2015, **101**, P. 258–263.
[15] Valeeva A.A., Rempel A.A., Gusev A.I. Two-sublattice ordering in titanium monoxide. *JETP Letters*, 2000, **71**, P. 460–464.
[16] Hall W.H. X-Ray Line Broadening in Metals. *Proc. Phys. Soc. London. Sect. A*, 1949, **62**, P. 741–743.
[17] Hall W.H., Williamson G.K. The Diffraction Pattern of Cold Worked Metals: I The Nature of Extinction. *Proc. Phys. Soc. London. Sect. B*, 1951, **64**, P. 937–946.
[18] Valeeva A.A., Petrovykh K.A., Schroettner H., Rempel A.A. Effect of stoichiometry on the size of titanium monoxide nanoparticles produced by fragmentation. *Inorganic Materials*, 2015, **51**, P. 1132–1137.
[19] Kohn W., Sham L.J. Self-Consistent Equations Including Exchange and Correlation Effects. *Phys. Rev. A*, 1965, **140**, P. 1133–1138.
[20] Jones R.O., Gunnarsson O. The density functional formalism, its applications and prospects. *Rev. Mod. Phys.*, 1989, **61**, P. 689–746.
[21] Perdew J.P., Burke K., Ernzerhof M. Generalized Gradient Approximation Made Simple. *Phys. Rev. Lett.*, 1996, **77**, P. 3865–3868.
[22] Giannozzi P., Baroni S., Bonini N. et al. Quantum espresso: a modular and open-source software project for quantum simulations of materials. *J. Phys. Condens. Matter*, 2009, **21**, 395502 (19 p.).
[23] Gusev A.I. Ordered Orthorhombic Phases of Titanium Monoxide. *JETP Letters*, 2001, **74**, P. 91–95.
[24] Payne M.C., Teter M.P., et al. Iterative minimization techniques for ab initio total-energy calculations: molecular dynamics and conjugate gradients. *Rev. Mod. Phys.*, 1992, **64**, P. 1045–1097.
[25] Andersson D.A., Korzhavyi P.A., Johansson B. Thermodynamics of structural vacancies in titanium monoxide from first-principles calculations. *Phys. Rev. B*, 2005, **71**, 144101 (12 p.).
[26] Graciani J., Mrquez A., Sanz J.F. Role of vacancies in the structural stability of α–TiO: A first-principles study based on density-functional calculations. *Phys. Rev. B*, 2005, **72**, 054117 (6 p.).
[27] Kostenko M.G., Lukoyanov A.V., Zhukov V.P., Rempel A.A. Vacancies in ordered and disordered titanium monoxide: Mechanism of B1 structure stabilization. *J. Sol. St. Chem.*, 2013, **204**, P. 146–152.
[28] Kostenko M.G., Lukoyanov A.V., Zhukov V.P., Rempel A.A. Effect of the long-range order in the vacancy distribution on the electronic structure of titanium monoxide $TiO_{1.0}$. *JETP Lett.*, 2012, **96**, P. 507–510.
[29] Kostenko M.G., Rempel A.A., Sharf S.V., Lukoyanov A.V. Simulation of the short-range order in disordered cubic titanium monoxide $TiO_{1.0}$. *JETP Lett.*, 2013, **97**, P. 616–620.